ISSN 1063-7745, Crystallography Reports, 2016, Vol. 61, No. 1, pp. 121–125. © Pleiades Publishing, Inc., 2016.
Original Russian Text © V.I. Petrenko, M.V. Avdeev, L.A. Bulavin, L. Almasy, N.A. Grigoryeva, V.L. Aksenov, 2016, published in Kristallografiya, 2016, Vol. 61, No. 1, pp. 132–137.

DIFFRACTION AND SCATTERING OF NEUTRONS

Effect of Surfactant Excess on the Stability of Low-Polarity Ferrofluids Probed by Small-Angle Neutron Scattering

V. I. Petrenko[a,b], M. V. Avdeev[a], L. A. Bulavin[b], L. Almasy[c], N. A. Grigoryeva[d], and V. L. Aksenov[e,a]

[a] *Joint Institute for Nuclear Research, Dubna, Moscow oblast, Russia*
[b] *Taras Shevchenko National University of Kyiv, Kyiv, Ukraine*
[c] *Wigner Research Centre for Physics, Hungarian Academy of Science, Budapest, Hungary*
[d] *St. Petersburg State University, St. Petersburg, Russia*
[e] *Konstantinov Petersburg Nuclear Physics Institute, National Research Centre "Kurchatov Institute", Gatchina, Russia*
e-mail: vip@nf.jinr.ru

Received March 6, 2015

Abstract—The structures of ferrofluids (FFs) based on nonpolar solvent decahydronaphthalene, stabilized by saturated monocarboxylic acids with hydrocarbon chains of different lengths, C16 (palmitic acid) and C12 (lauric acid), with an excess of acid molecules, have been studied by small-angle neutron scattering. It is found that the addition of acid to an initially stable system with optimal composition leads to more significant structural changes (related to aggregation) than those observed previously for this class of FFs. A comparison of the influence of monocarboxylic acids on the stability of nonpolar FFs suggests that the enhancement of aggregation is much more pronounced in the case of palmitic acid excess. This fact confirms the conclusion of previous studies, according to which an increase in the hydrocarbon chain length in a saturated acid reduces the efficiency of the corresponding FF stabilization.

DOI: 10.1134/S1063774516010168

INTRODUCTION

Ferrofluids (FFs) are suspensions of magnetic nanoparticles about 10 nm in size. This size, on the one hand, provides sedimentation stability of FFs and, on the other hand, determines the single-domain state of magnetic nanoparticles, which manifests itself in their practically superparamagnetic behavior in an external magnetic field. The FF structure is of interest for both fundamental research and applications [1–3].

Because of the strong attraction between nanoparticles (magnetic dipole–dipole interaction and van der Waals interaction), which may lead to their aggregation, FFs must be stabilized. Surfactant layers adsorbed on the surface of magnetic particles are often used to this end. In FFs based on low-polarity solvents, the presence of single layers of surfactants leads to an increase in the average distance between particles and, correspondingly, the weakening of the magnetic dipole–dipole attraction. Under these conditions, the FF aggregation stability is determined to a great extent by the interaction between surfactant and solvent; therefore, one of the most important factors affecting FF stability is the concentration of surfactant molecules in solution. In practice, there is an optimal ratio of the contents of magnetic nanoparticles and surfactant, a deviation from which violates FF stability [2, 4–6]. Note that this problem is general for colloidal solutions [7–10]. If the number of stabilizer (surfactant) molecules is insufficient, the stability deteriorates because these molecules cannot completely cover the surface of magnetic nanoparticles. In the case of surfactant excess, the mechanism of stability deterioration is not so obvious. Previously, structural changes in FFs with different surfactant excesses were investigated by small-angle neutron scattering (SANS) in systems based on low-polarity solvents (benzene and decahydronaphthalene), where nanomagnetite (obtained by coprecipitation) was coated by monocarboxylic acids with different alkyl chain lengths and degrees of saturation (unsaturated oleic acid, C18; saturated myristic acid, C14) [5, 11–13]. The main observed changes were related to the interaction between free surfactants (monocarboxylic acids), which differed to a great extent from the interaction between surfactant molecules in pure solutions without magnetic particles [14]. The structure of complex (magnetite plus surfactant) particles and interaction between them did not change much up to 15 vol % excess surfactant. With a further increase in the excess

concentration above some critical value, the stability sharply deteriorated, which manifested itself in the coagulation of complex particles and precipitation of agglomerates.

In this study we analyzed the possibility of expanding the range of surfactant stabilizers for FFs. Specifically, we were interested in the effect of their excess above optimal concentration on the stability of low-polarity FFs. The main purpose was to reveal (using SANS) the structural changes caused by adding surfactants to initial highly stable solutions of magnetite nanoparticles coated by single adsorption layers of saturated monocarboxylic acids with hydrocarbon chains of different lengths (palmitic acid (PA), C16, and lauric acid (LA), C12) in decahydronaphthalene. The stabilization of FFs using these acids, along with saturated myristic acid [15], also provides highly stable concentrated systems; however, their stabilization efficiency is somewhat lower. The stabilization efficiency of a surfactant is considered to be a relative fraction of magnetite nanoparticles that are stabilized in solution under identical conditions for adding different surfactants during magnetite coprecipitation with subsequent magnetic decantation (placing a fluid in an inhomogeneous magnetic field in order to initiate agglomeration and precipitation of nonstabilized magnetite). Thus, to obtain the desired concentration of magnetic particles in the final system with a less efficient surfactant, one must use a larger number of redispersion cycles with magnetic decantation of initially deposited magnetite in the surfactant-containing mixture. As in the case with myristic acid, the stabilized size of magnetic nanoparticles in FFs with PA and LA is smaller than that obtained with commonly used oleic acid [15]. In the SANS experiments described below, we generally applied a deuterated solvent to provide a maximum neutron contrast with acid molecules and increase the signal-to-noise ratio by reducing the incoherent background from hydrogen.

EXPERIMENTAL

Magnetite/palmitic acid/decahydronaphthalene and magnetite/lauric acid/decahydronaphthalene FFs with magnetite volume fractions $\varphi_m = 7.3$ and 8.9 vol %, respectively, and chemically pure LA and PA were supplied by the Center for Fundamental and Advanced Technical Research, Romanian Academy–Timisoara Branch. In the case of optimal stabilization of FFs of this type, almost all surfactant molecules existing in solution are adsorbed on the surface of magnetic nanoparticles; i.e., the concentration of free nonadsorbed surfactant in the FF volume is extremely low [16, 17]. To prepare samples without surfactant excess, initial FFs were diluted with protonated ($C_{10}H_{18}$) or deuterated ($C_{10}D_{18}$) decahydronaphthalene to $\varphi_m = 0.75$ vol %. This concentration was chosen so as to exclude the influence of particle–particle interaction (structural factor effect) on small-angle scattering. Samples with surfactant excess were prepared by adding a certain amount of acids and deuterated decahydronaphthalene $C_{10}D_{18}$ (99%, Deutero GmbH) to the corresponding initial concentrated FFs to obtain the magnetic material concentration $\varphi_m = 0.75$ vol % in the systems under study and the same content (90 vol %) of deuterated solvent in all samples. The volume fraction of excess surfactant in the FFs stabilized by LA and PA varied in the ranges to 10 and 5 vol %, respectively. SANS experiments were performed on the SANS-II facility at the Laboratory of Neutron Scattering of the Paul Scherer Institute (Villigen, Switzerland). The differential scattering cross section per sample unit volume (below, scattering intensity $I(q)$) was measured as a function of scattering vector modulus $q = (4\pi/\lambda)\sin(\theta/2)$, where λ is the neutron wavelength and θ is the scattering angle. Measurements were performed at room temperature. The separately measured scattering signal of the solvent was subtracted from the primary curves. To plot scattering curves in absolute units, we performed calibration using distilled water in a flat quartz cell with a neutron path length of 1 mm.

RESULTS AND DISCUSSION

Experimental SANS curves for diluted FFs without surfactant excess (Fig. 1) are described well within the model of noninteracting polydisperse particles of the "core–shell" type, which was previously used repeatedly for the FFs of this class [5, 11–13, 18–21]:

$$I(q) = I(0)\frac{\int_{R\min}^{R\max} D_n(r)\left[V(r)F(qr) + \eta V(r+\delta)F(q(r+\delta))\right]^2 dr}{\int_{R\min}^{R\max} D_n(r)\left[V(r) + \eta V(r+\delta)\right]^2 dr} + I_{bkg}, \quad (1)$$

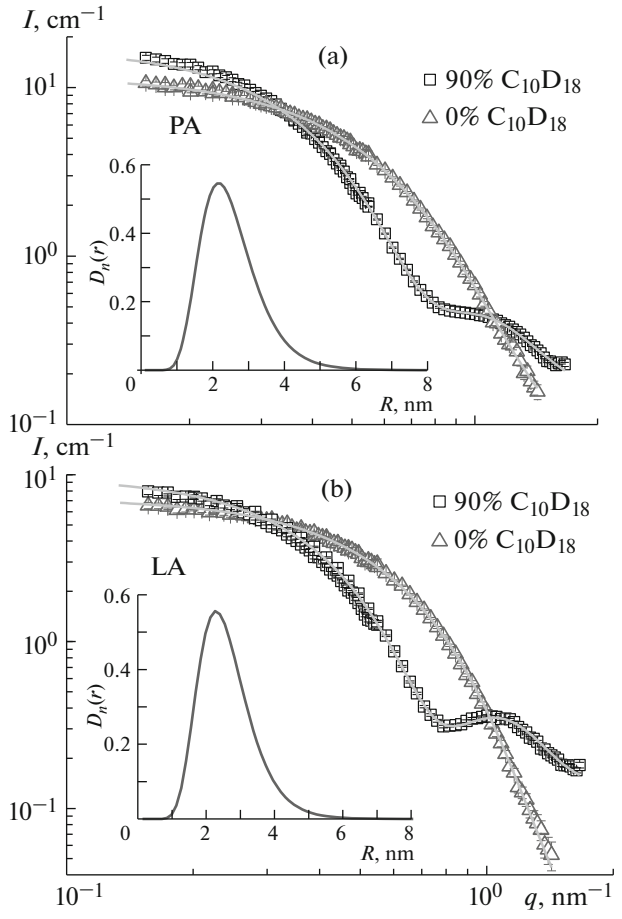

Fig. 1. Experimental SANS curves for the initial FFs diluted to φ_m = 0.75 vol %: (a) magnetite/PA/decahydronaphthalene and (b) magnetite/LA /decahydronaphthalene; (□) FFs with dominant content of deuterated decahydronaphthalene (90% $C_{10}D_{18}$), (Δ) FFs based on protonated decahydronaphthalene (0% $C_{10}D_{18}$), and (solid lines) curves approximated using the "core–shell" model (1). The insets show the size distribution functions for magnetite particles.

where

$$I(0) = \frac{\varphi_m}{\int_{R_{\min}}^{R_{\max}} D_n(r)V(r)dr} \times (\rho_0 - \rho_1)^2 \int_{R_{\min}}^{R_{\max}} D_n(r)[V(r) + \eta V(r+\delta)]^2 dr \quad (2)$$

is the intensity scattered into zero angle; $\eta = (\rho_1 - \rho_s)/(\rho_0 - \rho_1)$, is the contrast parameter, determined by the scattering length densities of magnetic-nucleus, ρ_0, surfactant shell, ρ_1, and liquid medium, ρ_s; $V(r) = 4/3\pi r^3$ is the volume of a sphere with radius r; δ is the thickness of stabilizing surfactant shell; $F(qr) = 3[\sin(qr) - qr\cos(qr)]/(qr)^3$ is the form factor of a sphere with radius r; $D_n(r) = \exp[-\ln(r/R_0)^2/2S^2]/(\sqrt{2\pi}Sr)$ is a lognormal-type size distribution function with the most probable radius R_0 and standard deviation S; $R_{\min}$ and $R_{\max}$ are, respectively, the minimum and maximum radii of FF magnetic particles (were fixed to be 1 and 14 nm in fitting); and I_{bkg} is the residual (after subtracting the solvent contribution to scattering) incoherent background. Fitting was performed by varying parameters $I(0)$, R_0, S, δ, and I_{bkg}.

The parameters of size distribution functions $D_n(r)$ in simultaneous approximation of data according to formula (1) for FF samples with contents of deuterated component in the solvent of 0 and 90 vol % were found to be $R_0 = 2.4(3)$ nm and $S = 0.32(3)$ for the PA-stabilized samples and $R_0 = 2.5(5)$ nm and $S = 0.29(3)$ for the LA-stabilized samples. The corresponding plots are shown in Fig. 1 (insets). Surfactant shell thickness δ (mainly for deuterated solvent) for the two stabilization versions (PA and LA) was approximately the same: $\delta = 2.0 \pm 0.8$ nm. The surfactant shell thickness is indistinguishable for the two acids because of the rather large error (~40%), which is explained by the very high sensitivity of parameter δ to the SANS curve discontinuity and to the residual background [22]. Within the error, the thickness is comparable with the results of previous studies on similar FFs [15]. In a protonated solvent, the contribution of the surfactant shell to scattering is small because of the minimum contrast between the surfactant and solvent.

The changes in the SANS curves for FFs with surfactant excess are shown in Fig. 2. The logic of previous studies [5, 11–13] of the structural changes in highly stable solutions of magnetite nanoparticles in dependence of the acid concentration was based on the following algorithm. The parameters of particle-size distribution function $D_n(r)$ and thickness δ of surfactant shell were obtained by approximating the curves for a given FF without acid excess. Then these parameters were fixed when fitting the experimental curves for the FF samples with acid excess, and a term describing the scattering from free surfactant was introduced into formula (1). Because of the small volume of acid molecules (in comparison with FF particles), this term had the form of the Guinier formula (see expression (3) below). When analyzing the scattering from FF particles, it was necessary to correct contrast taking into account the presence of free surfactant caused by the surfactant excess in the FF.

In this study, the algorithm [5, 11–13] turned out to be invalid to obtain adequate approximating curves within the modified model of noninteracting spherical particles in the presence of free surfactant. The reason is the existence of small (but sufficient to violate the model) structural instability of FF, which manifests itself in the formation of aggregates even at very small

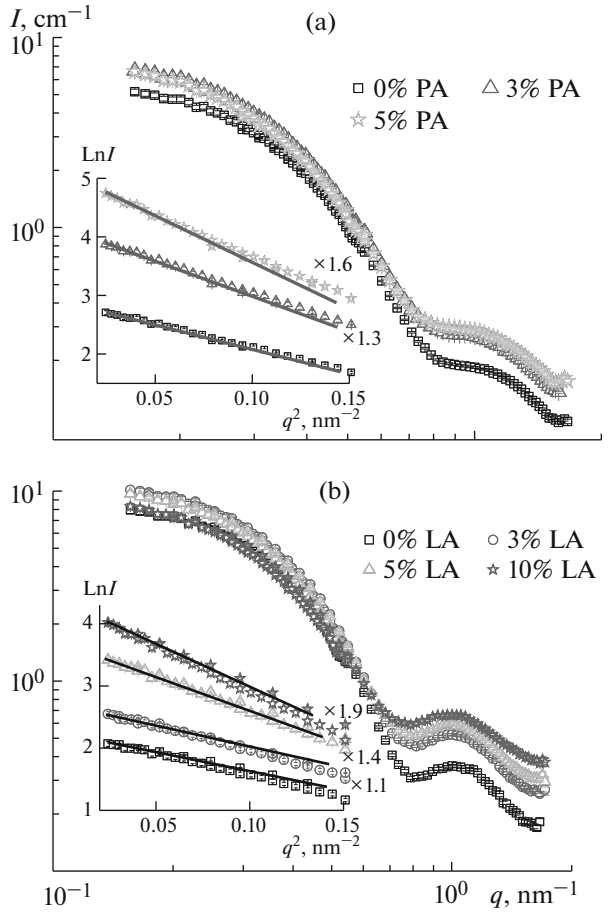

Fig. 2. Experimental SANS curves for the FFs based on decahydronaphthalene (90 vol % deuterated solvent) with different excesses (indicated in vol %) of (a) PA and (b) LA. The inset shows Guinier plots for all aforementioned systems. For better perception, some curves are multiplied by certain factors (indicated on the right).

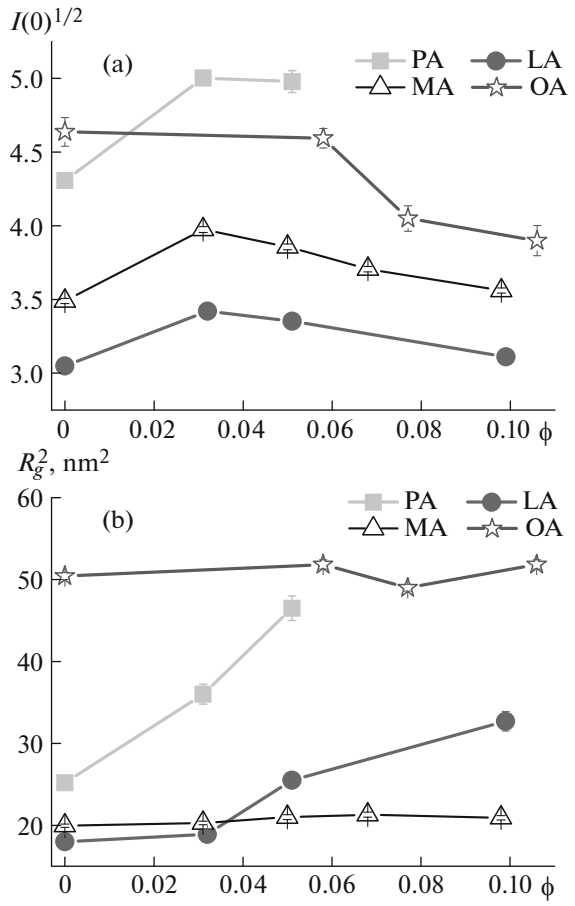

Fig. 3. Dependences of the Guinier parameters on the excess (volume fraction φ) of PA and LA: (a) intensity scattered into zero angle and (b) radius of gyration. Similar dependences, plotted from the data of [12, 13] for decahydronaphthalene-based FFs stabilized by oleic acid (OA) and myristic acid (MA), are shown for comparison.

additives of excess surfactant to solutions. Indeed, the standard approximation of the initial portions of experimental curves (at $q \leqslant 0.38$ nm^{-1}) by the Guinier law

$$I(q) = I(0)\exp\left(-R_g^2 q^2/3\right) \quad (3)$$

yields mean size characteristics: intensity scattered into zero angle, $I(0)$, and radius of gyration R_g, which are determined by the corresponding averagings over squared volume in a polydisperse system [16]. The theoretical curves derived from expression (3) are shown in Fig. 2 (insets). The changes in the Guinier-function parameters (zero-angle scattering intensity $I(0)$ and radius of gyration R_g) for the FFs with surfactant excess are presented in Fig. 3. For comparison, Fig. 3 shows also similar dependences of $I(0)$ and R_g, plotted based on data of [12, 13] for FFs in decahydronaphthalene, stabilized by oleic and myristic acids with the same content of deuterated solvent in solutions. Both parameters increase upon an initial excess of LA and PA; this increase is more pronounced in the samples stabilized by PA. Parameter $I(0)$ decreases with an increase in the free-surfactant fraction (Fig. 3a). According to formula (2), this is explained by the decrease in the contrast of complex particles (magnetite/monocarboxylic acid) caused by the growth of the concentration of hydrogen-containing acids molecules in the solvent. Parameter R_g continues to rise (Fig. 3b), which indicates the enhancement of aggregation. Comparing the behavior of R_g for FFs stabilized by different acids, one can conclude that, in contrast to the fluids stabilized by oleic and myristic acids, the systems under consideration (stabilized by LA and PA) exhibit a much lower structural stability in the presence of surfactant excess. Thus, a clear correlation is observed between the stabilizing efficiency of the acids used and the FF stability in the presence of surfactant excess: the more efficiently a surfactant

stabilizes magnetic particles in a fluid, the more stable the FF is under surfactant excess.

The effect revealed can be explained by the presence of two competing contributions to the stabilizing efficiency of monocarboxylic acids. It is known [4] that the main parameter determining the steric repulsion of magnetic nanoparticles in an FF is the surfactant shell thickness, which is proportional to the alkyl chain length. In this context, the chain length in LA (C12) is insufficient to provide stabilization of this kind. An additional factor affecting the repulsion between particles is the elastic properties of the shell (i.e., the ability of the shells of FF particles penetrate each other and be deformed under contact) [17]. The extended anisotropic structure of saturated-acid molecules leads to a peculiar organization of surfactant on the magnetite surface, which deteriorates the elastic properties of the shell and weakens repulsion. This effect manifests itself during stabilization by PA (C16); it is in agreement with the fact that the lowest efficiency of stabilizing magnetic nanoparticles in FFs is observed for stearic acid with a chain length of C18 (among other saturated monocarboxylic acids). Thus, an FF stabilized by myristic acid (having an intermediate chain length, C14) remains most stable under surfactant excess. In this context, its behavior is close to that of FFs stabilized by unsaturated oleic acid, which exhibits the highest stabilizing efficiency.

CONCLUSIONS

Based on SANS data, we obtained structural parameters of FFs (magnetite in decahydronaphthalene) stabilized by PA and LA at optimal surfactant content and at surfactant excess in solutions. It was shown that the size of surfactant molecule significantly affects the FF structure and stability. It was found that surfactant excess leads to larger structural changes in FFs (due to aggregation) than those observed previously for similar FFs stabilized by saturated myristic acid and unsaturated oleic acid. Among the systems studied, the enhancement of aggregation at surfactant excess is most pronounced for the PA-stabilized samples. The results of this study indicate a correlation between the stabilizing efficiency of the acids used and the stability of FFs with surfactant excess: the higher the surfactant efficiency is, the more stable the system is at surfactant excess.

ACKNOWLEDGMENTS

We are grateful to researchers from the Center for Fundamental and Advanced Technical Research (Timisoara, Romania) for supplying samples of initial ferrofluids.

This study was supported by the Russian Foundation for Basic Research, project no. 14-22-01113/14-ofi_m.

This work is based on experiments performed at the Swiss spallation neutron source SINQ, Paul Scherrer Institute, Villigen, Switzerland.

REFERENCES

1. B. Berkovski, *Magnetic Fluids and Applications Handbook* (Beggel House, New York, 1996).
2. L. Vekas, M. V. Avdeev, and D. Bica, *Magnetic Nanofluids: Synthesis and Structure in Nanoscience in Biomedicine,* Ed. by D. Shi (Springer, Berlin, 2009), Ch. 25, p. 650.
3. U. Häfeli and M. Zborowski, J. Magn. Magn. Mater. **321**, 1335 (2009).
4. R. E. Rosensweig, *Ferrohydrodynamics* (Cambridge Univ. Press, Cambridge, 1985).
5. V. I. Petrenko, M. V. Avdeev, V. L. Aksenov, et al., J. Surf. Invest. X-ray, Synchr. and Neutron Techniques **3** (1), 161 (2009).
6. D. Bica, Roman. Rep. Phys. **47**, 265 (1995).
7. P. Izquierdo, J. Esquena, Th. F. Tadros, et al., Langmuir **18**, 26 (2002).
8. A. B. Jódar-Reyes, A. Martín-Rodríguez, and J. L. Ortega-Vinuesa, J. Colloid. Interface Sci. **298**, 248 (2006).
9. V. L. Alexeev, J. Colloid. Interface Sci. **206**, 416 (1998).
10. J. Bibette, D. Roux, and B. Pouligny, J. Phys. II France **2**, 401 (1992).
11. V. I. Petrenko, M. V. Avdeev, V. L. Aksenov, et al., Solid State Phenom. **152–153**, 198 (2009).
12. A. V. Nagornyi, V. I. Petrenko, L. A. Bulavin, et al., Phys. Solid State **56** (1), 91 (2014).
13. L. A. Bulavin, A. V. Nagornyi, V. I. Petrenko, et al., Ukr. J. Phys. **58** (12), 1143 (2013).
14. V. I. Petrenko, M. V. Avdeev, L. Almásy, et al., Colloid. Surf. A **337**, 91 (2009).
15. M. V. Avdeev, D. Bica, L. Vekas, et al., J. Colloid. Inter. Sci. **334**, 37 (2009).
16. M. V. Avdeev and V. L. Aksenov, Phys. Usp. **53**, 971 (2010).
17. V. L. Aksenov, M. V. Avdeev, A. V. Shulenina, et al., Crystallogr. Rep. **56** (5), 792 (2011).
18. J. Wagner, J. Appl. Crystallogr. **37**, 750 (2004).
19. M. Kammel, A. Hoell, and A. Wiedenmann, Scr. Mater. **44**, 2341 (2001).
20. A. Hoell, M. Kammel, A. Heinemann, and A. Wiedenmann, J. Appl. Crystallogr. **36**, 558 (2003).
21. A. Hoell, R. Muller, A. Wiedenmann, and W. Gawalek, J. Magn. Magn. Mater. **252**, 92 (2002).
22. A. V. Nagornyi, V. I. Petrenko, M. V. Avdeev, et al., J. Surf. Invest. X-ray, Synchr. and Neutron Techniques **7** (1), 99 (2013).

Translated by Yu. Sin'kov